

199304710

128

N93-18899

52-13

[Handwritten signature]

P. 12

Precision X-band Radio Doppler and Ranging Navigation: Mars Observer Interplanetary Cruise Scenario

J. A. Estefan and S. W. Thurman
Navigation Systems Section

This article describes an error covariance analysis based on a Mars Observer mission scenario; the study was performed to establish the navigation performance that can potentially be achieved in a demonstration of precision two-way X-band (8.4-GHz) Doppler and ranging with the Mars Observer spacecraft planned for next year, and to evaluate the sensitivity of the predicted performance to variations in ground system error modeling assumptions. Orbit determination error statistics computed for a 182-day Doppler and ranging data arc predicted Mars approach orbit determination accuracies of about 0.45 μ rad in an angular sense, using a conservative ground system error model as a baseline. When less-conservative error model assumptions were employed, it was found that orbit determination accuracies of 0.19 to 0.30 μ rad could be obtained; the level of accuracy of the assumed Mars ephemeris is about 0.11 μ rad. In comparison, Doppler-only performance with the baseline error model was predicted to be about 1.30 to 1.51 μ rad, although it was found that when improved station location accuracies and Global Positioning System-based tropospheric calibration accuracies were assumed, accuracies of 0.44 to 0.52 μ rad were predicted. In the Doppler plus ranging cases, the results were relatively insensitive to variations in ranging system and station delay calibration uncertainties of a few meters and tropospheric zenith delay calibration uncertainties of a few centimeters.

I. Introduction

The Mars Observer (MO) spacecraft was launched on September 25 of this year and is the first of a series of planetary observer missions to be flown to the inner planets and small bodies of the Solar System, using modified versions of existing Earth-orbiting spacecraft [1]. MO carries an X-/X-band (7.2-GHz uplink/8.4-GHz downlink) transponder and is the first interplanetary spacecraft to rely solely

on a single-frequency X-band telecommunications system.¹ The MO mission will provide another opportunity to test the range data filtering technique that proved to be very successful in recent demonstrations utilizing S-/S-band

¹ P. B. Esposito, S. W. Demcak, D. C. Roth, W. E. Bollman, and C. A. Halsell, *Mars Observer Project Navigation Plan*, Project Document 642-312, Rev. C (internal document), Jet Propulsion Laboratory, Pasadena, California, June 15, 1990.

(2.1-GHz uplink/2.3-GHz downlink) ranging data from Galileo [2] and S-/X-band (2.1-GHz uplink/8.4-GHz downlink) ranging data from Ulysses [3,4].

Two-way ranging has been an operational data type for interplanetary spacecraft navigation for many years. Past mission experience has been that ranging data cannot be utilized at their inherent accuracy due to the influence of small unmodeled spacecraft nongravitational forces caused by attitude control thruster firings and other spacecraft activity. In addition, inconsistent and unreliable station delay calibrations often precluded the effective use of precise ranging. In this article, it will be shown that for the MO spacecraft's approach to Mars, notable orbit determination accuracies can be achieved with X-band Doppler and ranging by taking advantage of relatively recent improvements in the consistency and accuracy of station delay calibrations. These improvements, coupled with explicit modeling of spacecraft nongravitational forces and residual station delay calibration errors, should make it possible to utilize MO ranging data at or near their inherent accuracy, even for data arcs much longer than those used in the recent demonstrations.

II. Orbit Determination Error Analysis

The Orbit Analysis and Simulation Software set (OASIS/314) was used to perform the error covariance analysis. The numeric qualifier represents the JPL Navigation Systems Section (314) version of this software, which was modified extensively by A. S. Konopliv to support interplanetary work. The original version of OASIS was designed for Earth orbiter systems error analysis.

A. Earth-to-Mars Interplanetary Cruise

MO's interplanetary cruise has been segmented by the MO Navigation Team into five independent phases, each ending prior to a planned trajectory correction maneuver. The strategy assumed for analysis purposes, as described in the MO Navigation Plan,² was to simulate n days of data for each individual phase and determine the spacecraft state vector at the initial epoch of each phase, along with the remaining error model parameters and their associated uncertainties.³ The error statistics were then propagated, or mapped, to the time of encounter and displayed in a target-centered aiming plane ("B-plane") coordinate system, which is defined in the Appendix.

The MO trajectory segment selected for this analysis was the fourth phase (184-day interval), which represents

the longest leg of the interplanetary cruise and has the most stringent orbit determination accuracy requirements, in order to support the final trajectory correction maneuver prior to Mars orbit insertion. The analysis corresponds to an injection epoch of September 16, 1992, the first date of the 20-day launch window. The focus of more recent orbit determination analyses has been the last date of the launch window, October 5, 1992; however, the first date was chosen for ease of reference to results presented by Esposito, et al.⁴ in which initial conditions at the earlier date of the launch window are provided.

B. Radio Metric Data Acquisition Strategy

Using a nomenclature in which I = injection, E = encounter, and T_0 = epoch time, two-way Doppler and range data were simulated from T_0 = February 7, 1993, 00:00:00.000 UTC (I + 143) to I + 325 days (E - 12 days) and were assumed to have been acquired from the Deep Space Network's 34-m high-efficiency (HEF) subnet. From I + 143 to E - 90 days, Doppler and range data were acquired during a daily tracking pass. From E - 90 to E - 30 days, two passes of Doppler and range data were acquired on a daily basis, and from E - 30 to E - 12 days, Doppler and range data were acquired continuously. In all cases, the Doppler and range data were sampled at a rate of 1 point every 10 min, or 6 points/hr.

To account for data noise, the Doppler were weighted (an assumed random measurement uncertainty was chosen) at a $1\text{-}\sigma$ uncertainty of 0.032 mm/sec over a 600-sec integration time (equivalent to a 0.1-mm/sec weight for a 60-sec integration time) or "deweighted" to 0.32 mm/sec in some cases. A 60-sec Doppler weight of 0.1 mm/sec is believed to be near the true inherent accuracy of the data at X-band (8.4 GHz). It is not expected that the Doppler data quality will significantly degrade during the cruise phase, as the first solar conjunction does not occur until December 12, 1993, several months after encounter.⁵ The Doppler data weight was adjusted by an elevation-dependent function (to reduce the weight of the low-elevation data) at each station, and data points below a 10-deg elevation were omitted. A similar approach was used for the range data, which were weighted at a $1\text{-}\sigma$ uncertainty of 10 m or, in some cases, 1 m.

C. Navigation Error Modeling

In this subsection, the modeled parameters are broken down into two categories: estimated and considered; random data noise characteristics, which were described

² Ibid.

³ Ibid.

⁴ Ibid.

⁵ Ibid.

previously, are summarized in Table 1 along with all the estimated and considered parameters and their associated a priori uncertainties. Modeling assumptions are described below.

1. Estimated Parameters. The estimated parameters include state variables to account for mismodeling of spacecraft nongravitational (NG) accelerations induced by environmental disturbances, such as solar radiation pressure (SRP), as well as spacecraft self-induced perturbing forces, such as gas leaks from valves and pressurized tanks, attitude thruster misalignments, and/or angular momentum desaturation burn mismodeling. These parameters, together with random biases representing station delay calibration errors and other uncalibrated delays in the range measurements, were estimated along with the spacecraft trajectory by using a batch-sequential, factorized Kalman filter.

For the MO SRP model, an area-to-mass ratio of $17.0 \text{ m}^2/2328.8 \text{ kg}$ was assumed. Three nondimensional coefficients representing a simple spacecraft bus model (G_r, G_x, G_y) were estimated, with a priori uncertainties equivalent to 10 percent of their maximum attainable values (see Table 1). In a recently published MO interplanetary cruise error analysis,⁶ a much more sophisticated SRP model was employed and will probably be used during the operational phase of the mission. Although the model used in this analysis is simplistic, it does provide a reasonable standard of comparison with the earlier studies.⁷ Spacecraft nongravitational accelerations in each spacecraft body-fixed axis were modeled as estimated stochastic parameters. A three-parameter, first-order Markov colored noise model (exponentially correlated process) was used, with steady-state sigmas of $3 \times 10^{-12} \text{ km/sec}^2$, and time constants (correlation times) of 1 day, with a 1-day batch size. The random bias parameters representing ranging system calibration errors on the data were also estimated as stochastic parameters with a correlation time of zero and a steady-state sigma equal to an a priori offset calibration uncertainty of 5 m or 2 m in some cases. A separate range bias parameter was modeled for each station pass and a 1-day batch size assumed.

2. Considered Parameters. Recall that a considered parameter is treated by the filter as an unmodeled systematic error and may significantly affect the error statistics

of the estimated parameter set. The total error covariance, or full-consider covariance, accounts for the effects of considered parameter uncertainties as well as the formal covariance computed by the filter, so as not to understate the predicted navigation performance. The considered parameters used in this study account for systematic errors in the Earth-Mars ephemerides, Mars' Newtonian gravitational parameter (GM), DSN station locations, tropospheric calibration data, and ionospheric calibration data.

The error covariance from planetary ephemeris DE234 was chosen to account for the Earth-Moon barycenter and Mars ephemeris errors. The 12×12 formal error covariance matrix gives errors in the six Brouwer and Clemence Set III orbital elements of the Earth-Moon system and the six elements of Mars. The formal covariance was scaled by a factor of 2, as suggested by its creators, to reflect a more realistic assessment of the errors.⁸ Uncertainty of the Mars GM value was taken to be $0.15 \text{ km}^3/\text{sec}^2$, or about 3 parts in 10^6 .

Station location uncertainties include both a relative component and an absolute (geocentric) component. The relative component refers to DSN site-to-site uncertainty, which is measured accurately by very long baseline interferometry (VLBI); the geocentric component refers to a common error in locating the DSN sites with respect to the Earth's center of mass (VLBI is insensitive to this component). Two station location covariances for the DSN HEF stations (DSS's 15, 45, and 65) were used for this analysis: Moyer's LS234IP station location covariance,⁹ and Folkner's MO station location covariance.¹⁰ In the case of LS234IP, the formal covariance representing spin radius and longitude errors were scaled by a factor of 5 and 2.5 (in sigma), respectively, as suggested by Moyer.¹¹ For Folkner's set, which is based on VLBI and lunar laser ranging (LLR) data, the formal covariance was scaled by a factor of 2 (in sigma) to give realistic station-to-station uncertainties comparable with differences derived independently from satellite laser ranging (SLR) and VLBI. The formal covariance was also inflated to account for

⁶ D. C. Roth, "Orbit Determination Results for Planetary Protection Analysis (5 OCT 92 Launch Date)," JPL Interoffice Memorandum NAV-92-007 (internal document), Jet Propulsion Laboratory, Pasadena, California, April 15, 1992.

⁷ Esposito, Demcak, Roth, Bollman, and Halsell, *op. cit.*

⁸ E. M. Standish, "The JPL Planetary Ephemerides, DE234/LE234," JPL Interoffice Memorandum 314.6-1348 (internal document), Jet Propulsion Laboratory, Pasadena, California, October 8, 1991.

⁹ T. D. Moyer, "Station Location Set LS234IP for Planetary Ephemeris DE234," JPL Interoffice Memorandum 314.5-1588 (internal document), Jet Propulsion Laboratory, Pasadena, California, November 20, 1991.

¹⁰ W. M. Folkner, "DE234 Station Locations and Covariance for Mars Observer," JPL Interoffice Memorandum 335.1-92-013 (internal document), Jet Propulsion Laboratory, Pasadena, California, May 26, 1992.

¹¹ Moyer, *op. cit.*

geocenter offset between LLR and SLR measurements, radio-planetary frame-tie uncertainty, and Earth orientation mismodeling.¹² Table 1 provides the absolute and relative uncertainties in station cylindrical coordinates for both station location sets.

Wet and dry components of the tropospheric path delay calibration error were considered with $1\text{-}\sigma$ zenith uncertainties of 4 cm and 1 cm, respectively, based on present-day accuracy of adjustments to a seasonal model. In some cases, Global Positioning System (GPS)-based calibrations were assumed to be available, with a total $1\text{-}\sigma$ zenith delay uncertainty of 2 cm. The model used for ionospheric refraction is described by Wu [5]. For this analysis, a $1\text{-}\sigma$ zenith electron content uncertainty of 5×10^{16} elec/m² was assumed and is representative of current DSN calibration capability using ground-based observations of GPS satellites.

III. Accuracy Assessment

The filter-generated computed covariance was combined with consider parameter sensitivities in order to construct the full-consider covariance, which was then mapped to encounter (August 19, 1993, 12:48:08.000 ET) and displayed in Mars-centered aiming plane (“B-plane”) coordinates, referred to the Mars Mean Equator of Date. In some instances, the mapped computed-only statistics are tabulated along with the full-consider statistics for comparison of “filter-world” versus “real-world” results.

A. Doppler-Only Performance

The baseline case for Doppler-only analysis, utilizing the conservative error model described in the previous section (LS234IP station location covariance and present tropospheric calibration accuracy), and assuming a Doppler weight of 0.1 mm/sec (60-sec count time), yields aiming plane dispersions equivalent to about $1.51 \mu\text{rad}$ in an angular sense (by comparison, the accuracy requirement for the fourth phase of the interplanetary cruise is about $0.5 \mu\text{rad}$ ¹³). The statistical results for this case are given in Table 2, where SMAA and SMIA denote the semi-major and semi-minor axes of the dispersion ellipse, respectively; θ denotes the orientation of the dispersion ellipse, measured clockwise from the horizontal axis of the aiming plane; and LTOF denotes the linearized time-of-flight uncertainty. The Doppler data in this case exhibited a very high sensitivity to station location uncertainty,

which was about 1.5 m (Doppler data are nearly insensitive to z -height errors). In an initial attempt to reduce this sensitivity, the Doppler data were “deweighted” by an order of magnitude, to a value of 1.0 mm/sec. This reduced the aiming plane dispersions by about 30 percent, and the time-of-flight uncertainty by about 20 percent; the angular accuracy for this case was about $1.10 \mu\text{rad}$. When the baseline Doppler-only case (0.1-mm/sec weight) was repeated with the Folkner station location covariance, the aiming plane dispersions and time-of-flight uncertainty were reduced by about a factor of 2 relative to the baseline case, which corresponded to an angular accuracy of about $0.67 \mu\text{rad}$. If it was assumed that GPS-based calibrations of the troposphere were used in addition to the Folkner station covariance, the aiming plane dispersions and time-of-flight uncertainty were further reduced by about 22 percent, yielding an angular accuracy on the order of $0.52 \mu\text{rad}$. These results suggest that the full benefit of X-band Doppler can only be realized with Earth platform (station locations and Earth orientation) calibration accuracies of about 15 cm, and centimeter-level zenith tropospheric calibration accuracies.

B. Doppler Plus Range

When ranging data were included along with the Doppler data, the results improved substantially over those obtained in the Doppler-only cases. Statistical results for these cases are given in Table 3. Use of the conservative baseline error model (10-m range weight and a 5-m a priori range bias uncertainty for each station pass) resulted in an angular accuracy of about $0.50 \mu\text{rad}$. As with the Doppler-only results, the use of an improved zenith tropospheric delay calibration value did not significantly improve performance in this case; however, when Folkner’s improved station location covariance was utilized, much better performance was obtained, with improvements in the aiming plane dispersions on the order of 40 percent and time-of-flight uncertainty of about a factor of 2. The use of the improved GPS calibrations of the troposphere together with Folkner’s station covariance resulted in only about an additional 7- to 9-percent improvement.

In an attempt to further reduce the data sensitivity to systematic error sources, the Doppler measurements were deweighted by an order of magnitude, with mixed results (see Table 3). Another case was evaluated in which the a priori uncertainties for the range bias parameters were reduced to 2 m, which should be achievable for X-band ranging data. Here, only a slight improvement in overall performance was observed; a different result from that witnessed in the Galileo and Ulysses precision ranging demonstrations, in which shorter data arcs were assumed [2-4].

¹² Folkner, *op. cit.*

¹³ P. Esposito, personal communication, Mars Observer Navigation Team Chief, Navigation Systems Section, Jet Propulsion Laboratory, Pasadena, California, March 1992.

C. Doppler Plus High-Precision Range

Recent experiments by T. P. McElrath using S-/X-band two-way ranging data obtained from Ulysses near the spacecraft's recent Jupiter encounter have met with remarkable success using range data weights of 2 m [4]. With a 2-m range weight, a substantial improvement in orbit determination performance was obtained for Ulysses over orbit solutions computed with 10-m and 5-m range weights; an earlier analysis indicated that it should be possible to weight X-/X-band ranging data at 1 m or better [3]. To predict the potential performance of high-precision ranging for MO, an additional set of cases was calculated using a range weight of 1 m and assumed a priori range bias uncertainties of 2 m. The results obtained for these cases are provided in Table 4. For the case in which the Folkner station location covariance was used, orbit determination accuracies of 0.19 to 0.30 μ rad were predicted; by comparison, the level of accuracy of the assumed Mars ephemeris is about 0.11 μ rad. The use of an improved GPS-based tropospheric calibration accuracy produced no noticeable change, as shown in Table 4. One final case was computed (not shown in the table) using the Folkner station location covariance, GPS-based tropospheric calibration accuracy, and a priori range bias uncertainties of 5 m; once again, no noticeable change in the aiming plane dispersions was observed. It is interesting to observe that the use of an order-of-magnitude improvement in the range data noise value did not result in a dramatic improvement over the the 10-m range case, except when the Doppler data were deweighted to 1.0 mm/sec. This is consistent with the fact that the a priori range measurement biases, used at their current level, impose a limit on the ability of the range data to provide a greater share of the information content over the "tight" (0.1-mm/sec) Doppler.

Figures 1 and 2 provide a graphical comparison of the aiming plane statistics (dispersion ellipses and uncertainty in time-of-flight) for the three primary data strategies addressed in this article: Doppler-only navigation, Doppler plus 10-m range navigation, and Doppler plus high-precision (1-m) range navigation. Each result is representative of the improved orbit determination error model which incorporates Folkner's station location covariance and GPS-based tropospheric calibrations. The improvement of the Doppler plus range orbit solutions over

the Doppler-only result is clearly evident in the illustrations.

IV. Discussion

There are some subtle differences in terms of modeling and data acquisition strategies between the analysis described in this article and the recent interplanetary cruise error analysis performed by the MO Navigation Team.¹⁴ As alluded to earlier, a more sophisticated SRP model was mechanized in the Navigation Team's analysis, which will be a good candidate for use in mission operations. For completeness, the analysis provided here could be revisited by using the more realistic model. Also, the first day of the 20-day launch window was used in this analysis versus the last day of the 20-day launch window. This is such a short interval of time relative to the interplanetary cruise phase selected for this study that the differences are considered insignificant for covariance analysis purposes. Additionally, the data cutoff for the navigation team's study was E-25 days versus E-12 days assumed herein.

V. Conclusions

The results of the error covariance analysis predicts that Doppler-based orbit solutions for MO will be much more sensitive to Earth platform and transmission media calibration errors than solutions derived from both Doppler and ranging data. The Doppler and ranging cases analyzed herein also showed that orbit solutions using high-precision (meter-level) ranging data appear to be nearly insensitive to variations in ranging system and station delay calibration errors of a few meters, and tropospheric calibration uncertainties of a few centimeters at zenith. Not studied here was the potential performance of precise to highly precise radio Doppler and ranging navigation resulting from improved data noise characteristics and a priori uncertainties of the range measurement biases. Whether these findings will be consistent with the results obtained with shorter (one-and-a-half to three-month) data arcs in the Galileo and Ulysses precision ranging demonstrations is yet to be determined.

¹⁴ D. C. Roth, op. cit.

Acknowledgment

The authors would like to thank V. M. Pollmeier for his helpful comments and suggestions in review of this article.

References

- [1] J. F. Jordan and L. J. Wood, "Navigation, Space Mission," *Encyclopedia of Physical Science and Technology*, New York: Academic Press, vol. 8, pp. 744–767, 1987.
- [2] V. M. Pollmeier and S. W. Thurman, "Application of High-Precision Two-Way Ranging to Galileo Earth-1 Encounter Navigation," *TDA Progress Report 42-110*, vol. April–June 1992, Jet Propulsion Laboratory, Pasadena, California, pp. 21–32, August 15, 1992.
- [3] S. W. Thurman, T. P. McElrath, and V. M. Pollmeier, "Short-Arc Orbit Determination Using Coherent X-band Ranging Data," paper AAS 92-109, AAS/AIAA Spaceflight Mechanics Meeting, Colorado Springs, Colorado, February 24–26, 1992.
- [4] T. P. McElrath, B. Tucker, K. E. Criddle, P. R. Menon, and E. S. Higa, "Ulysses Navigation at Jupiter Encounter," paper AIAA 92-4524 (in press), AIAA/AAS Astrodynamics Conference, Hilton Head, South Carolina, August 10–12, 1992.
- [5] S. C. Wu, "Atmospheric Media Effects on ARIES Baseline Determination," *TDA Progress Report 42-103*, vol. July–September 1990, Jet Propulsion Laboratory, Pasadena, California, pp. 61–69, November 15, 1990.

Table 1. Assumed orbit determination modeling errors.

Source	A priori uncertainty, 1σ	Remarks
Random data noise		
Two-way Doppler (60-sec average)	Baseline, 1.0 mm/sec Precise, 0.1 mm/sec	
Two-way range	Baseline, 10 m Precise, 1 m	
Estimated parameters		
Spacecraft state vector	Position, 10^5 km Velocity, 1 km/sec	Loose knowledge
SRP constant coefficients (percent of nominal value)	$G_r = 10$ percent (= 0.13) $G_x = 10$ percent (= 0.01) $G_y = 10$ percent (= 0.01)	Radial and lateral components
Estimated stochastic parameters		
Spacecraft self-induced accelerations	Radial, 3×10^{-12} km/sec ² Lateral, 3×10^{-12} km/sec ²	τ (correlaton time) = 1 day
Range biases (1 per station pass)	Baseline, 5 m Precise, 2 m	τ (correlaton time) = 0
Considered parameters		
Mars planetary ephemeris (geocentric)	Radial, 0.4 km Down track, 30 km Normal, 48 km	JPL ephemeris DE234 (scaled by 2-in. sigma)
Mars GM	$0.15 \text{ km}^3/\text{sec}^2$	Conservative
DSN station coordinates baseline (LS234IP)	Spin radius, 0.84 m Longitude, 0.47 m z-height, 9.99 m	Relative uncertainties between stations ≈ 10 cm
Precise (Folkner)	Spin radius, 0.18 m Longitude, 0.19 m z-height, 0.22 m	Relative uncertainties between stations $\approx 3-5$ cm
Tropospheric zenith delay calibration error	4 cm (wet) 1 cm (dry)	
GPS-based tropospheric calibration error	2 cm (total)	
Ionospheric zenith electron content calibration error (at "ionospheric bulge")	$5 \times 10^{16} \text{ e/m}^2$	

Table 2. 1- σ aiming plane statistics for DSN Doppler-only navigation.

SMAA, ^a km	SMIA, ^b km	θ , deg	LTOF ^c sec
Baseline case (LS234IP station covariance)			
64	38	164	14 ^d
515	119	25	187
Folkner station covariance			
226	81	25	82
Folkner station covariance with GPS tropospheric calibrations			
177	77	28	64
Baseline case with GPS tropospheric calibrations			
495	117	25	180
Baseline case with deweighted Doppler			
279	104	50	96 ^d
372	136	43	144

^a Semi-major areas.

^b Semi-minor areas.

^c Linearized time-of-flight.

^d Computed-only results.

Table 3. 1- σ aiming plane statistics for DSN Doppler plus range navigation.

SMAA, km	SMIA, km	θ , deg	LTOF, ^a sec
Baseline case (LS234IP station covariance)			
27	0.06	64	5.8 ^a
169	1.9	64	65
Folkner station covariance			
99	1.2	64	32
Folkner station covariance with GPS tropospheric calibrations			
92	1.1	64	29
Baseline case with GPS tropospheric calibrations			
165	1.9	64	64
Baseline case with deweighted Doppler			
167	0.29	64	35 ^a
187	1.7	64	43

^a Computed-only results.

Table 4. $1\text{-}\sigma$ aiming plane statistics for DSN Doppler plus high-precision range navigation.

SMAA, km	SMIA, km	θ , deg	LTOF, ^a sec
Baseline case (LS234IP station covariance)			
26	0.06	64	5.6 ^a
154	2.0	64	60
Folkner station covariance			
92	1.2	64	30
Folkner station covariance with GPS tropospheric calibrations			
87	1.1	64	27
Baseline case with GPS tropospheric calibrations			
150	1.9	64	59
Baseline case with deweighted Doppler			
81	0.15	64	17 ^a
118	1.7	63	29

^a Computed-only results.

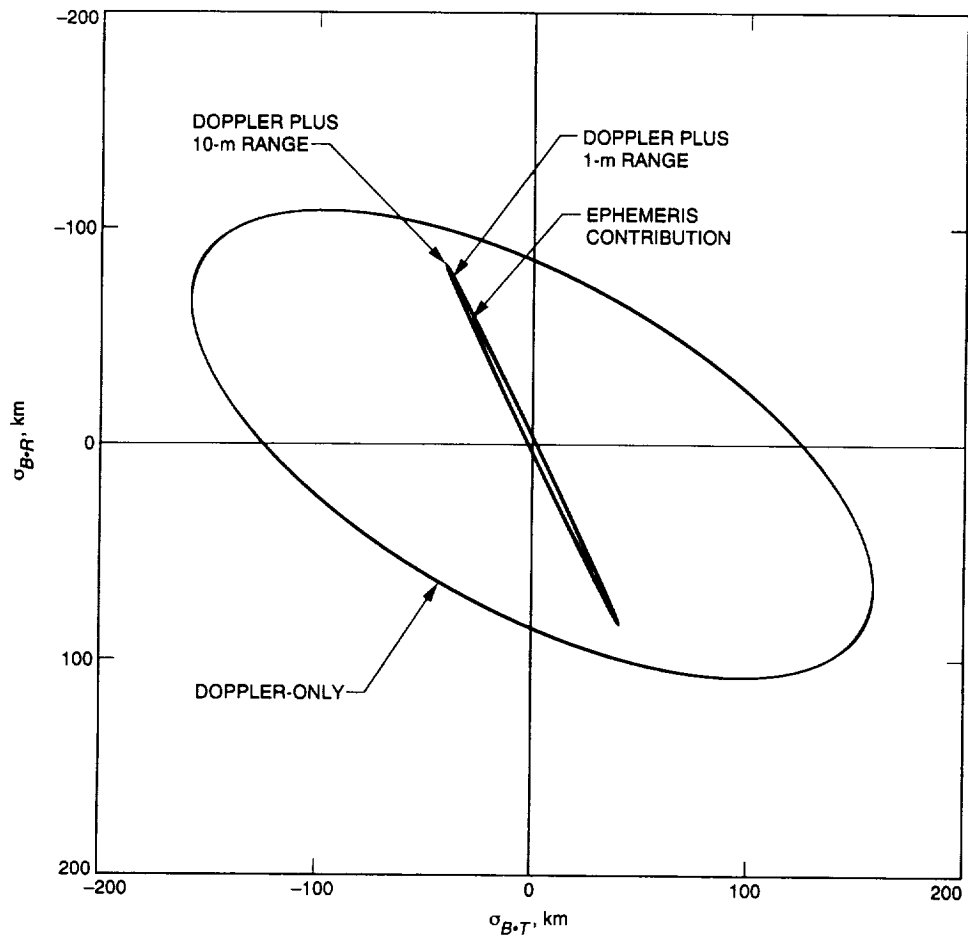


Fig. 1. Aiming plane dispersion ellipses for different data strategies.

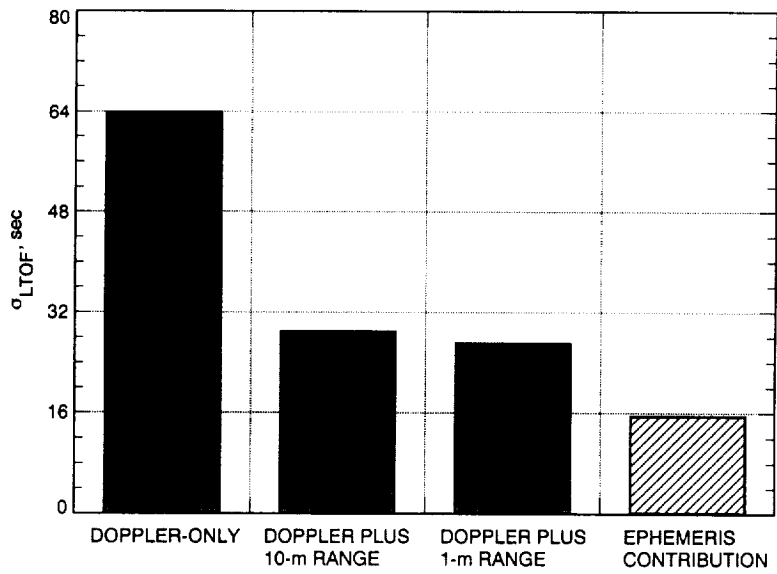


Fig. 2. Uncertainty in linearized time-of-flight (LTOF) for different data strategies.

Appendix

Planetary approach trajectories are typically described in aiming plane coordinates, often referred to as “B-plane” coordinates (see Fig. A-1). The origin of this system is the center of the target body. The encounter parameters are defined in terms of the orthogonal unit vectors \hat{S} , \hat{T} , and \hat{R} . The \hat{S} vector is parallel to the incoming asymptote of the approach hyperbola, while \hat{T} is normally specified to lie in the ecliptic plane (the mean plane of the Earth’s orbit); \hat{R} completes the triad. (In this particular analysis, the \hat{T} unit vector was defined to lie in the Martian equatorial plane.) The aim point is specified by the miss vector, \vec{B} ,

which locates where the point of closest approach would be if the target planet had no mass and did not deflect the flight path; the time from encounter (point of closest approach) is defined by the LTOF, which specifies what the time of flight to encounter would be if the magnitude of the miss vector were zero. Orbit determination errors are characterized by a $1\text{-}\sigma$ or $3\text{-}\sigma$ B-plane dispersion ellipse, also shown in Fig. A-1, and the $1\text{-}\sigma$ or $3\text{-}\sigma$ uncertainty in LTOF. In Fig. A-1, SMAA and SMIA denote the semi-major and semi-minor axes of the dispersion ellipse, respectively.

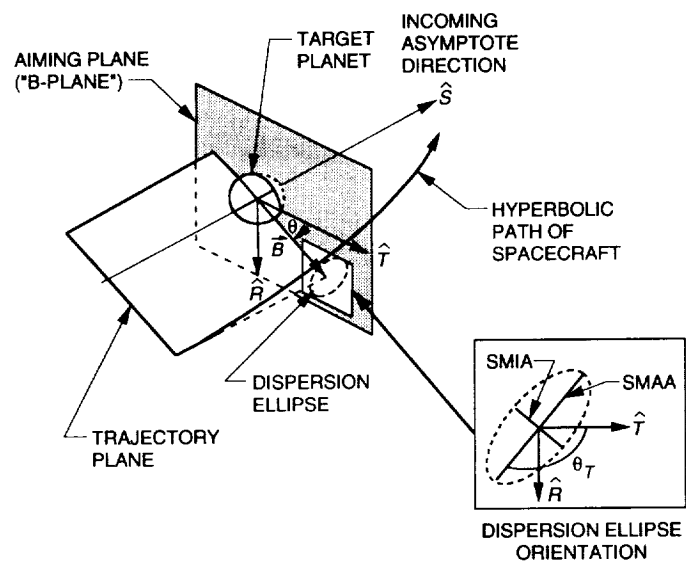


Fig. A-1. Aiming plane coordinate system definition.